

EXPERIMENTAL INVESTIGATION OF EFFECTS OF BUOYANCY ON SUPERCRITICAL CARBON DIOXIDE HEAT TRANSFER IN ROUND TUBES

Sandeep Pidaparti

Graduate Research Assistant
Georgia Institute of Technology
Atlanta, Georgia
spidaparti3@gatech.edu

Devesh Ranjan

Associate Professor
Georgia Institute of Technology
Atlanta, Georgia
devesh.ranjan@me.gatech.edu

Mark Mikhaeil

Graduate Research Assistant
Georgia Institute of Technology
Atlanta, Georgia
mmikhaeil3@gatech.edu

Mark Anderson

Research Professor
University of Wisconsin
Madison, Wisconsin
manderson@enr.wisc.edu

Jacob McFarland

Associate Professor
University of Missouri
Columbia, Missouri
Jacob.a.mcfarland@gmail.com

ABSTRACT

A series of integral experiments were performed to investigate the unusual heat transfer characteristics to supercritical carbon dioxide flowing in round tubes under constant heat flux boundary condition. Wall temperatures were measured over a range of experimental parameters that varied fluid inlet temperature from 20 – 55° C, operating pressure from 7.5 to 10.2 MPa, mass flux from 150 to 350 Kg/m²s and a maximum heat flux of 62.5 KW/m². Measurements were made for horizontal, upward, and downward flows to study the effect of buoyancy and flow acceleration caused by drastic density variation. Existing criterion to predict the influence of buoyancy suggested that the experimental data can be classified into three regimes namely normal, deteriorated, and enhanced heat transfer. In the case of upward flow, severe localized deterioration in heat transfer was observed due to reduction in the turbulent shear stress and is characterized by sharp increase in wall temperature. In the case of downward flow, turbulent shear stress is enhanced by the buoyancy forces leading to enhanced heat transfer. In the case of horizontal flow, flow stratification occurred leading to a circumferential variation in wall temperature. Thermocouples mounted 180° apart on the tube revealed that the wall temperatures on the top side are significantly higher than the bottom side of the tube. When the bulk temperature is greater than the pseudocritical temperature, normal heat transfer was observed irrespective of flow orientation indicating that the buoyancy effects are negligible.

INTRODUCTION

As the traditional sources of energy used for power generation (natural gas, coal, oil etc) begin to deplete their costs will continue to rise. Hence, there is a need for alternative sources (nuclear, wind, solar etc) of energy and improvements in the thermal efficiency of the power generation. As a member of Generation-IV International Forum (GIF), the Department of Energy (DOE) has undertaken leading role in this area by funding research related to supercritical fluids both for reactor coolants (supercritical water) and for advanced power generation (supercritical carbon dioxide power cycle) [1]. It has been shown recently that the supercritical water-cooled (SCW) nuclear power plants can achieve higher efficiencies compared to the current generation nuclear power plants. Additionally, they also decrease the capital and operational costs of the plant [2]. However, one of the biggest challenges in SCWR development is reactor core design as no reliable data is currently available to model heat transfer from reactor fuel bundles to the

reactor coolant (water). The main objective of this study is to understand the unusual heat transfer phenomenon to supercritical fluids flow in circular tube and develop correlations to accurately model the same. These results can later be extended to model the fuel bundles. Carbon dioxide is used as the working fluid as it has much lower critical temperature and pressure compared to water, and also carbon dioxide exhibits similar thermophysical property variations near a pseudo-critical temperature.

Carbon dioxide enters into the supercritical state at a pressure of 7.38 MPa and temperature of 31.1^o C. In the supercritical region, any fluid experience significant property variations and for carbon dioxide these variations are presented in figure 1 in terms of normalized units.

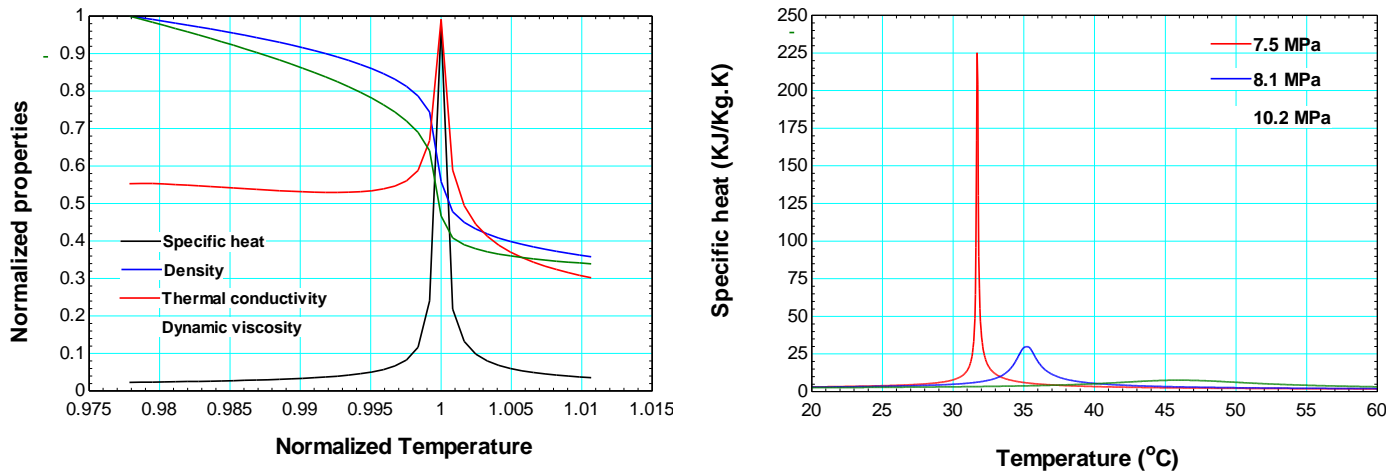


Figure 1. Variation of thermophysical properties of CO₂ in the supercritical region

It can be seen that for every pressure in the supercritical region, there exists a local peak in specific heat at the temperature known as pseudocritical temperature. Below the pseudocritical temperature, the fluid resembles a liquid and beyond this temperature it resembles a dense gas. These drastic variations in properties broaden out with increase in operating pressure.

Using the National Institute of Science and Technology (NIST) REFPROP database, the pseudocritical temperature for carbon dioxide can be defined as,

$$T_{pc} = -122.6 + 6.124p - 0.1657p^2 + 0.01773p^{2.5} - 0.0005608p^3 \quad (1)$$

Where T_{pc} is in °C and pressure, p , is in bars.

Crossing the pseudocritical line, the fluid does not experience any distinct phase change and hence, phenomena such as critical heat flux are not applicable anymore. However, at supercritical conditions, deteriorated heat transfer regime may still exist and the conditions for which deterioration occurs needs to be identified.

EXPERIMENTAL FACILITY

The schematic of the experimental facility is shown in figure 2. The key components of the loop are labeled in the figure.

System is pressurized by a Scientific Systems, Inc. SFC-24, positive displacement, constant pressure HPLC pump (S10SNXP1). It is capable of pressurizing the system to 10,000 *psi* with an accuracy of ±2% of full scale. A buffer tank of volume (~0.5 *m*³) is installed in the loop to increase the system volume and minimize the variable fluctuations in the loop.

The main driving pump is a Micropump (GLH25-JVSE-CH15 316 SS) magnetically driven gear pump. It is capable of handling flow rates between 0.6-7.0 *GPM*, a differential pressure of 125 *psi*, and a maximum operating pressure of 1500 *psi*. This pump is coupled to Baldor variable frequency drive (VSIST41-0), and this in conjunction with a throttling valve is used to precisely control the mass flow rate in the loop.

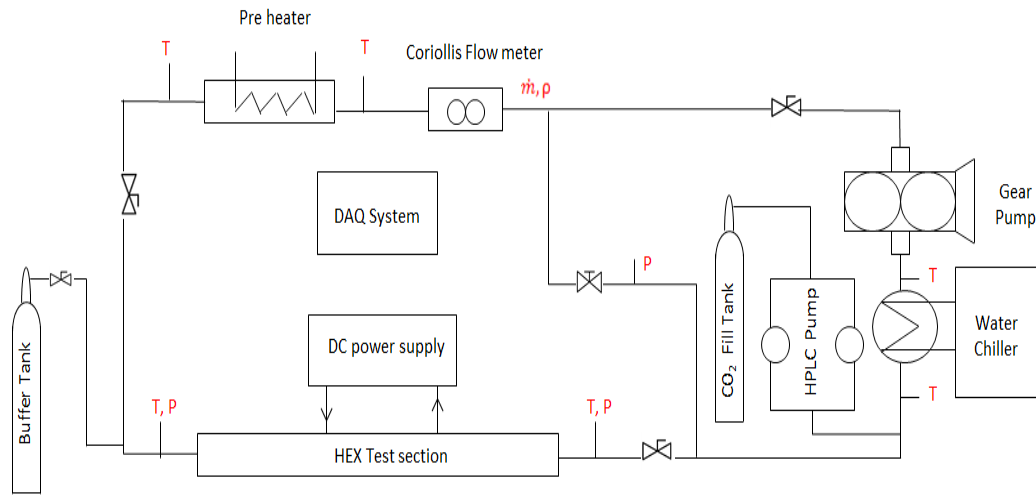


Figure 2. Schematic of the experimental facility

A Micro Motion Coriolis flow meter (F025P319CCAAEZZZZ) and transmitter (2700I12ABAEZZZ) are used to measure the mass flow rate in the system. The flow meter is capable of measuring flow rates up to 0.27 Kg/s with a $\pm 0.1\%$ full-scale accuracy. Measurements from the flow meter as a feed-back control for the variable frequency drive.

Temperatures in the loop excluding the test section were controlled using a high pressure CO₂ preheater and pre-cooler. In the preheater, CO₂ splits into two tubes that run next to a 5.5 KW cartridge heater. This preheater is used to raise the temperature of CO₂ to the desired test section inlet temperature. Upon exiting the test section, the CO₂ enters into a high pressure pre-cooler where excess heat is removed facilitating the pump to move liquid like CO₂. The pre-cooler is a concentric tube-in-tube heat exchanger where the chilled water runs through the outside and the CO₂ through the inside tube. Chilled water is provided using Advantage Engineering (M1-1.5A) water chiller with a maximum cooling capacity of 1.5 refrigeration tons. Inlet and outlet temperatures to the test section are measured by Omega 3 wire platinum RTDs having maximum uncertainty of $\pm 0.3^{\circ}$ C. These RTDs are calibrated against the boiling water and ice bath to quantify the systematic error. The pressure is monitored by Omega gauge pressure transducers (PX309-3KGSV) with a manufacturer specified accuracy of $\pm 0.25\%$ of full scale. Several K-type thermocouples are used in the loop to monitor the amount of energy that was being put in or removed from the flow by each component.

The test section is a stainless steel 316 circular pipe with 0.5" OD, 0.43" ID, and is 1m long. Constant heat flux boundary condition is provided to the test section using a Magna-Power electronics TSD10-500/480 DC power supply. The heat flux to the test section is varied by adjusting the voltage between copper clamped terminals at the ends. The accuracy of voltage control is $\pm 0.01\%$ of full scale and current control is $\pm 0.04\%$ of full scale. The test section is electrically and thermally insulated from rest of the loop by using Swagelok dielectric fittings at each end of the test section.

Outer wall temperatures of the test section are measured using 20 E type stick on thermocouples. Out of these 20 thermocouples, 10 thermocouples are mounted on the top side and 10 on the bottom side at axial locations which are 75mm apart from each other. The first thermocouple is mounted at 300mm from the inlet side to allow for the flow to be hydro-dynamically fully developed before heating starts. It should be noted that the perspective of top and bottom side is with respect to horizontal orientation of test section. These E-type thermocouples have manufacturer specified uncertainty of $\pm 0.1^{\circ}$ C or 0.4%, whichever is greater. Drift in wall thermocouples reading is minimized by performing specific insitu calibration under no heat flux conditions.

EXPERIMENTAL PROCEDURE AND DATA ANALYSIS

A series of integral experiments were performed by changing the mass flow rate and heat flux for operating pressures of 7.5, 8.1, and 10.2 MPa. The inlet temperature to the test section was varied from 20 to 55^o C to cover the whole range of bulk temperatures spanning the pseudocritical temperature. The mass flux was in the range of 150-350 Kg/m²s and the heat flux was in the range of 10-62.5 KW/m². Three different test section orientations; horizontal, upward and downward flow were investigated to understand the effects of buoyancy. During the experiment, all independent parameters such as test section inlet temperature, mass flow rate, pressure, and heat flux were monitored and controlled by NI Labview DAQ system. For each operating condition, the system was assumed to be at steady state once the energy balance on the system came within $\pm 10\%$. This involves calculation of the heat input by the preheater and the test section DC power supply, and the heat removed by the pre-cooler. Heat added, or removed to/from CO₂ in the preheater and pre-cooler was calculated by measuring the temperatures across each component and performing energy balance as,

$$Q_{CO_2} = \dot{m}(i_{in} - i_{out}) \quad (2)$$

Once the system achieves a steady state, the data was recorded for 500s at rate of 1 Hz and the average of these data points is used for the analysis.

Heat flux to the test section is estimated as,

$$Q_{PS}'' = \frac{V_{PS} I_{PS}}{\pi DL} \quad (3)$$

Outer wall temperatures are measured and inner wall temperatures are estimated using a simple one-dimensional, steady state heat conduction equation,

$$T_{wi} = T_{wo} + \frac{\dot{q}}{4k_{ss}} \left[\left(\frac{D_{out}}{2} \right)^2 - \left(\frac{D_{in}}{2} \right)^2 \right] - \frac{\dot{q}}{2k_{ss}} \left(\frac{D_{out}}{2} \right)^2 \ln \left(\frac{D_{out}}{D_{in}} \right) \quad (4)$$

Where, \dot{q} is the volumetric heat rate expressed as,

$$\dot{q} = \frac{V_{PS} I_{PS}}{\left[\frac{\pi}{4} (D_{out}^2 - D_{in}^2) L \right]} \quad (5)$$

Using the assumption of constant heat flux, the bulk temperature at the locations of the thermocouples was obtained by performing energy balance on a differential control volume in the test section, and using the following equation [4],

$$T_{b+1} = T_b + \frac{Q_{PS}''}{\dot{m} C_p} \pi D x \quad (6)$$

The local heat transfer coefficient is then defined as,

$$h = \frac{Q_{PS}''}{A(T_{wi} - T_b)} \quad (7)$$

Finally, the experimental local Nusselt number was determined as,

$$Nu_b = \frac{hD}{k_b} \quad (8)$$

UNCERTAINTY ANALYSIS

Using the method proposed by Kline and McClintock [5], the uncertainty in the measurement of the heat transfer coefficient can be expressed as follows,

$$\delta h = \left[\left(\frac{\partial h}{\partial Q_{PS}''} \delta Q_{PS}'' \right)^2 + \left(\frac{\partial h}{\partial T_{wi}} \delta T_{wi} \right)^2 + \left(\frac{\partial h}{\partial T_b} \delta T_b \right)^2 \right]^{0.5} \quad (9)$$

Evaluating the partial differentials in Eq. (9), relative uncertainty in the measurement of the heat transfer coefficient can be expressed as,

$$\frac{\delta h}{h} = \left[\left(\frac{\delta Q_{PS}''}{Q_{PS}''} \right)^2 + \left(\frac{\delta T_{wi}}{T_{wi} - T_b} \right)^2 + \left(\frac{\delta T_b}{T_{wi} - T_b} \right)^2 \right]^{0.5} \quad (10)$$

The uncertainty in measurement of the wall temperatures and the heat flux was described earlier. It is clear from Eq. (10) that as the wall temperature and bulk temperature approach each other the uncertainty in the measurement of heat transfer coefficient increases. This generally occurs close to the pseudocritical point at sufficiently high mass flow rate and low heat flux.

Use of dielectric fittings minimizes the heat loss from the test section to the rest of the loop and hence, the only source of heat loss is the natural convection from the outer tube to the atmosphere. The estimation of heat loss based on natural convection was less than 5% without insulation. The test section as well as the whole loop is well insulated with flexible ceramic fiber glass insulation and hence, the heat loss to the atmosphere is assumed to be negligible under such conditions and was not included in the uncertainty analysis.

RESULTS AND DISCUSSION

Effect of operating pressure

The effect of operating pressure was investigated by comparing the test results for downward flow at three different operating pressures, 7.5, 8.1, and 10.2 MPa, for a mass flux of 195 Kg/m²s, and a heat flux of 13.5 KW/m². The heat transfer coefficients and wall temperatures are plotted against the normalized bulk temperature as shown in Figure 3. It can be seen that the wall temperature increases as the operating pressure is increased.

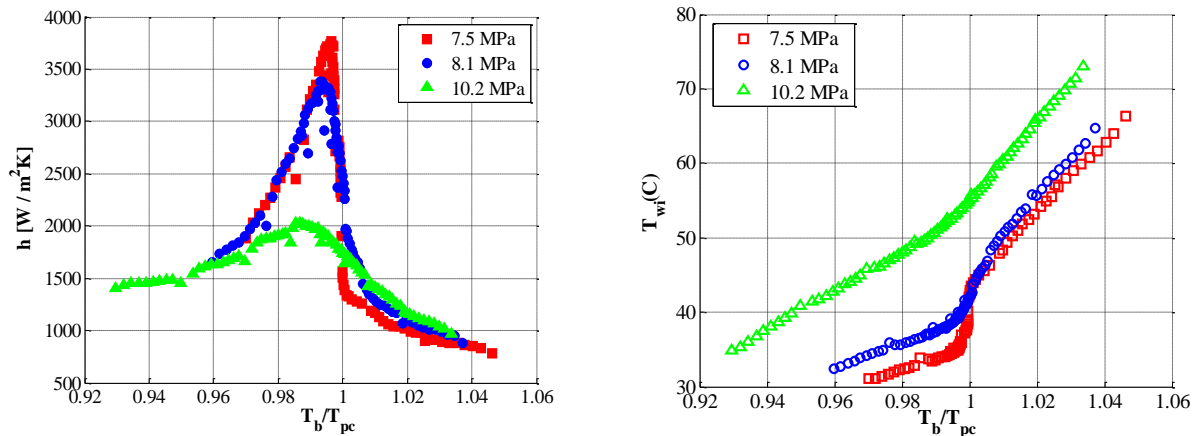


Figure 3. Effect of operating pressure on heat transfer for downward flow

When the bulk temperature (T_b) is lower than the pseudocritical temperature (T_{pc}), heat transfer coefficients are higher for the lower operating pressure with maximum enhancement observed slightly below the pseudocritical temperature. However, when the T_b is higher than T_{pc} , the heat transfer coefficients are higher for the higher operating pressures. This dependence of heat transfer coefficient on the pressure and temperature can be attributed to the variation of isobaric Prandtl number. These results were observed to be true for upward and horizontal flows as well provided that the heat flux is sufficiently high compared to the mass flux, and the buoyancy effects are negligible.

Effect of flow direction

In order to investigate the effect of buoyancy on heat transfer, the results at operating pressure of 10.2 MPa for horizontal, vertically upward, and downward flows are compared for a mass flux of 195 Kg/m²s, heat flux of 24 KW/m², and an inlet temperature of 46^o C. Figure 4 shows the variation of heat transfer coefficient and wall temperature along the length of the tube.

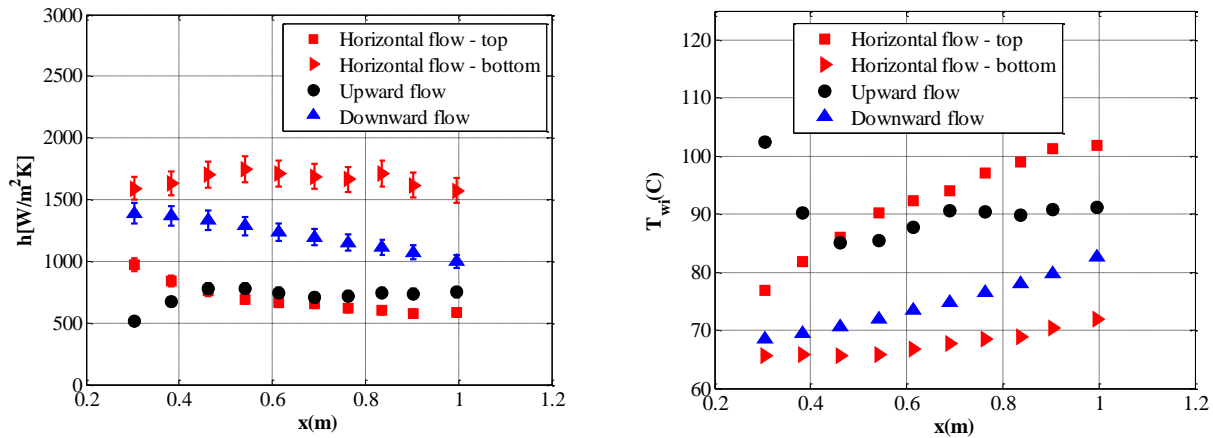


Figure 4. Effect of flow direction on heat transfer at operating pressure of 8.1 MPa

In the case of horizontal flow, it has been observed that the wall temperature on the top side are significantly higher than wall temperatures on the bottom side leading to a circumferential variation in the wall temperature. This was particularly true when $T_b < T_{pc} < T_w$. Under these conditions, the fluid density near the wall is significantly lower than the fluid density in the bulk of flow and, hence, the buoyancy effects become prominent. This density gradient causes the low density fluid to rise from the bottom side of the tube thereby, enhancing the heat transfer on the bottom side whereas the top side is covered by a blanket of fluid having low thermal conductivity deteriorating the heat transfer on the top side. This phenomenon has been experimentally observed in previous horizontal flow studies on supercritical water [6-8] and supercritical CO₂ [9]. The circumferential variation in wall temperature was observed to be more pronounced at low mass flux and high heat flux.

In the case of upward flow, localized peaks in the wall temperature were observed as can be seen from the wall temperature profile of upward flow in Figure 4. This severe localized deterioration was observed initially by Shitsman [10], Ackerman [11], and was originally believed to be similar to the film boiling phenomenon at subcritical pressures. However, experiments by [12], [13] showed occurrence of localized peaks even when the wall temperature is lower than the pseudocritical temperature. These conditions should result in a liquid like fluid blanket in the near wall-region and hence, doesn't support the theory of film boiling.

These localized peaks are often referred to as "buoyancy peaks" and occur as a result of modification of turbulent shear stress by the buoyancy forces acting on the flow [14]. It is believed that, as the fluid is heated along the tube, the density difference between the near wall region and bulk flow increases as a result of which the boundary layer experiences a buoyancy force due to its reduced density. In case of upward flow, this buoyancy force opposes the wall shear stress reducing the turbulence production in the law of wall region. As the boundary layer grows, for a particular boundary layer thickness, the wall shear stress will be balanced by the buoyancy force and at this point the bulk flow is decoupled from the wall causing the wall temperature to spike. As the buoyancy force increases further, a region of negative shear stress develops resulting in formation of a "M-shaped" velocity profile restoring turbulence production and hence, the wall temperature decrease after the spike. Experimental evidence of the "M-shaped" velocity profile was provided [15-18] using pitot tubes and micro thermocouples. Bourke and Pulling [16], showed formation of "M-shaped" profile after the spike in wall temperature, whereas Kurganov *et al* [18] found that the "M-shaped" profile occurred at the spike in wall temperature.

In the case of downward flow, the buoyancy force acts in the direction of wall shear stress increasing the turbulence production and thereby, enhancing the heat transfer compared to the cases where buoyancy is absent. As can be seen from Figure 4, wall temperatures for downward flow don't exhibit any localized peaks and are significantly lower than that of the upward flow.

Effect of inlet temperature

It is expected that the effect of buoyancy on heat transfer is influenced by the inlet temperature due to variation in both radial and axial properties. In order to investigate this effect, wall temperatures recorded for different inlet temperatures at operating pressures of 7.5 MPa, mass flux of 320 Kg/m²s, and heat flux of 24 KW/m² are compared. These plots are shown in Figure 5 for horizontal, upward, and downward flows.

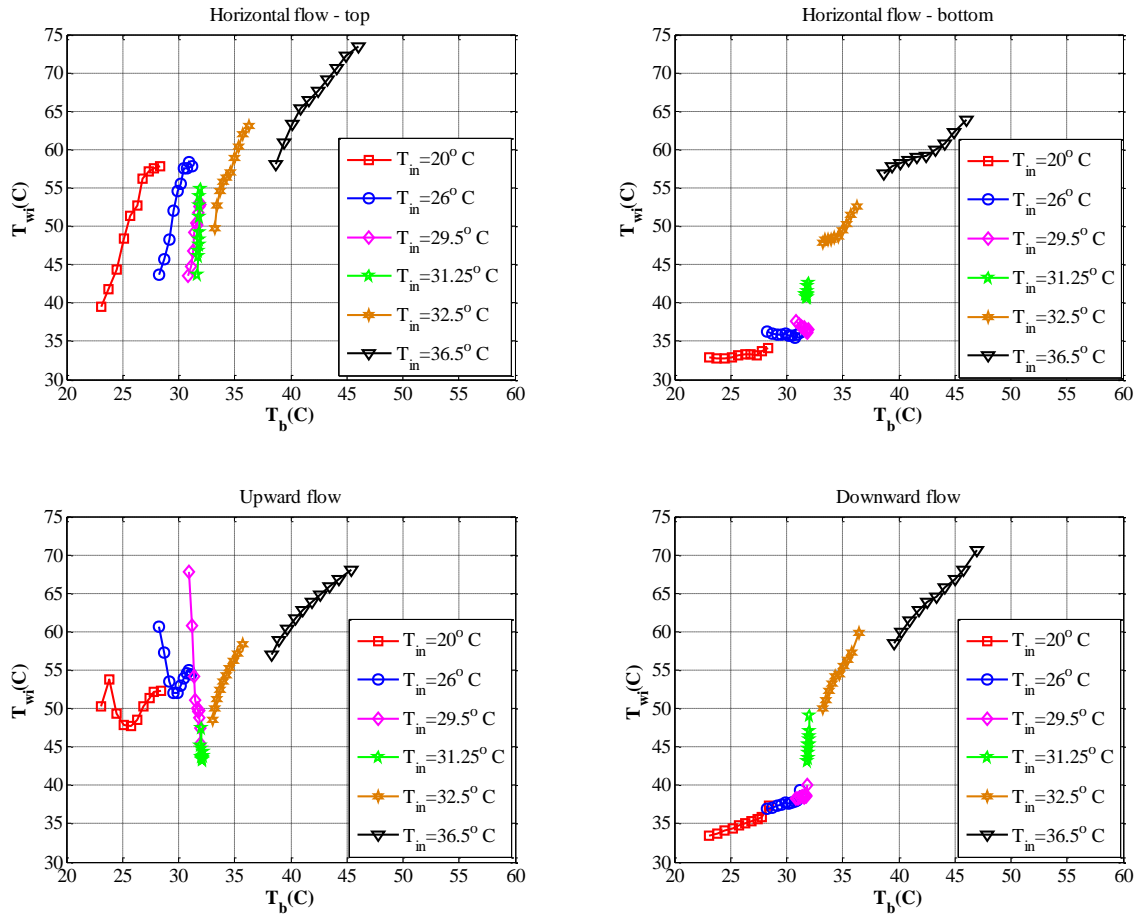


Figure 5. Effect of inlet temperature on the wall temperatures

In the case of horizontal flow, for inlet temperature below the pseudocritical temperature (for instance, $T_{in}=20^\circ\text{C}$), it has been observed that the wall temperatures on the top side are significantly higher than the wall temperatures on bottom side as discussed in the previous section. However, when the inlet temperature was raised above the pseudocritical temperature (for instance, $T_{in}=36.5^\circ\text{C}$), the difference between the top and bottom surface temperatures reduced as can be seen from Figure 5. This is because as the T_b moves away from the T_{pc} , the CO₂ bulk density nearly approaches the value of density at the wall and the buoyancy effects are minimized [8]. It is expected that with further increase in the inlet temperature, the temperature difference between top and bottom sides will nearly be zero. However, due to limitations of the current test facility this phenomenon couldn't be tested but was experimentally proven for supercritical water by Bazargan *et al* [8].

One more striking feature is that, as the inlet temperature is changed, severe discontinuity in the wall temperature was observed. This effect was more pronounced on the top side than on the bottom side. It is believed that this could be due to the effect of thermal entry length which is not well defined in the case of supercritical fluids. For a constant property fluid, thermal entry length is defined as the tube length

required to achieve constant radial temperature distribution. From this perspective, the thermal entry length in the case of supercritical fluids can be very long or in some cases impossible to achieve due to continuous radial and axial variation in thermophysical properties along the tube length [19]. The effect of thermal entrance length was less pronounced as the bulk temperature moves away from the pseudocritical temperature due to less variation in properties.

In the case of upward flow, sharp localized peaks are observed for inlet temperature below the pseudocritical temperature as discussed earlier. However, when the inlet temperature was raised above the pseudocritical temperature (for instance, $T_{in}=32.5^{\circ}C$), there was no evidence of localized peaks. In this case, the density of bulk CO_2 is nearly the same as density of CO_2 in the near wall region. As a result of this, the boundary layer doesn't experience any opposing buoyancy force and hence, the turbulence is not affected irrespective of flow direction. In fact, the wall temperatures for both upward and downward flows were observed to be similar as can be seen from Figure 5. It can also be seen that the location of localized peaks can be readily changed by varying the fluid inlet temperature [20-21]. For instance, spike in wall temperature for inlet temperature of $20^{\circ}C$ occurred at the location of second thermocouple whereas for inlet temperature of $26^{\circ}C$ it occurred at the location of first thermocouple. Hence, as the inlet temperature increases, the localized peaks in wall temperature appear to move towards the inlet of the tube. This can again be attributed to the thermal entrance length effects [20] and was observed to be true for all the test cases.

It is also interesting to note the steep increase in wall temperature in the case of downward flow for inlet temperatures close to the pseudocritical temperature. This was also observed on the bottom side of the tube in the case of horizontal flow under similar conditions. This could be due to a phenomenon which is similar to film boiling at subcritical pressures and is often referred to as "pseudo-film" boiling phenomenon in literature [11].

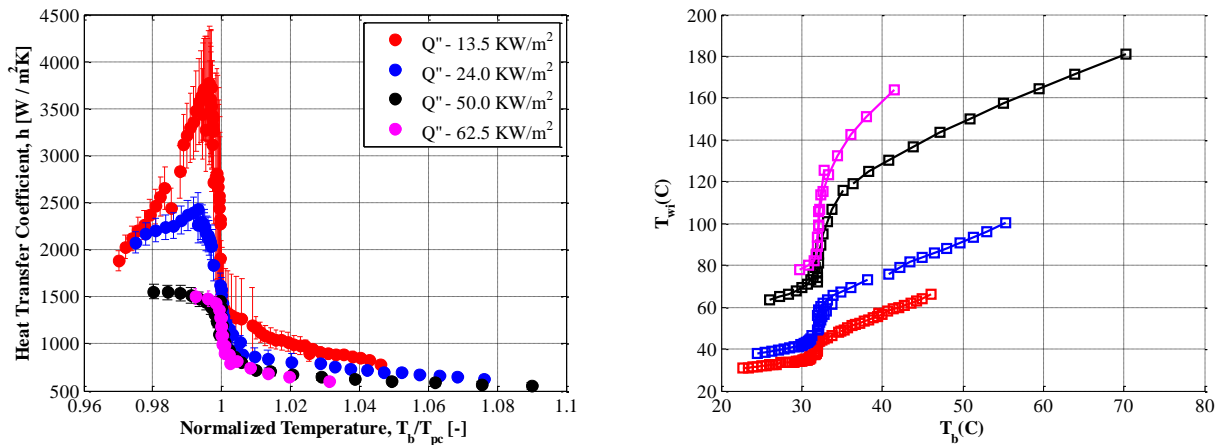


Figure 6. Effect of heat flux on heat transfer at an operating pressure of 7.5 MPa

Effect of heat flux

In order to investigate the effect of heat flux and the effect of pseudo-film boiling phenomenon further, tests were conducted for downward flow at operating pressure of 7.5 MPa, mass flux of 195 Kg/m²s for varying heat fluxes. The results are presented in Figure 6, in the form of the wall temperatures and heat transfer coefficients versus the bulk temperatures for different heat fluxes.

For low heat flux cases ($Q_{PS}'' = 13.5$, and 24 KW/m²), the energy input to the test section was not sufficient to span the pseudocritical region. As a result, inlet temperature was changed to span the pseudocritical region and hence, it was initially believed that the sharp increase in wall temperature is due to the thermal entrance length effects. However, for high flux cases ($Q_{PS}'' = 50$, and 62.5 KW/m²), the energy input to the test section is high enough to span the pseudocritical region and the sharp increase in wall temperature was still observed as can be seen from Figure 6. This indicates that the phenomenon is

due to pseudo-film boiling and not due to the thermal entrance length effects. It should also be noted that the heat transfer enhancement reduces with increase in heat flux. As the heat flux increases, the region of the maximum specific heat moves away from the boundary layer and hence, it is easier to overcome the region of highest specific heat. In other words, the area integrated values of specific heat decreases near the pseudocritical region causing a reduction in enhancement.

Buoyancy criteria

As seen in previous sections, the heat transfer to supercritical CO₂ is quite different than that of heat transfer to constant property fluids. One of the reasons for this unusual heat transfer can be associated with the effect of buoyancy due to large variations in axial and radial density profiles. Hence, it is important to identify the conditions for which the effects of buoyancy can safely be ignored. The effects of buoyancy can be effectively quantified based on Grashof number which represents the ratio of buoyancy forces to viscous forces and is defined as,

$$Gr = \frac{g\beta(T_w - T_b)d^3}{\nu_b^2} \quad (11)$$

Buoyancy parameters based on the variants of Grashof number are suggested in literature both for horizontal and vertical flows. In order to investigate the influence of buoyancy, experimentally determined Nusselt numbers are normalized with respect to Jackson's correlation [22] and compared with the existing buoyancy criteria. Jackson's correlation as shown in Eq. (12) is proven to best capture the heat transfer to S-CO₂ under forced convection conditions in the absence of buoyancy effects or any sort of deterioration.

$$Nu_{jackson} = 0.0183Re_b^{0.82}Pr_b^{0.5} \left(\frac{\rho_w}{\rho_b}\right)^{0.3} \left(\frac{c_{pav}}{c_{pb}}\right)^n \quad (12)$$

Where the subscript n is proposed as,

$$n = 0.4, \text{ for } T_b < T_w < T_{pc} \text{ and } 1.2T_{pc} < T_b < T_w$$

$$n = 0.4 + 0.2 \left(\frac{T_w}{T_{pc}} - 1\right), \text{ for } T_b < T_w < T_{pc}$$

$$n = 0.4 + 0.2 \left(\frac{T_w}{T_{pc}} - 1\right) \left(1 - 5 \left(\frac{T_b}{T_{pc}} - 1\right)\right), \text{ for } T_{pc} < T_b < 1.2T_{pc}$$

Jackson [21] suggested a buoyancy parameter, Bu , for vertical flows which was derived from boundary layer theory taking into account the property variations:

$$Bu = C_B B_o_b F_{VP1} F_{VP3} F_{VP4} \quad (13)$$

Corresponding terms in Eq. (13) are defined as,

$$B_o_b = \frac{Gr_b}{Re_b^{2.625} Pr_b^{0.4}}$$

$$F_{VP1} = \left(\frac{\mu_{av}}{\mu_b}\right) \left(\frac{\rho_{av}}{\rho_b}\right)^{-0.5}$$

$$F_{VP3} = \left(\frac{Pr_{av}}{Pr_b}\right)^{-0.4}$$

$$F_{VP4} = \frac{\rho_b - \rho_{av}}{\rho_b - \rho_w}$$

It was suggested that for C_B value of 4600, the flow can be assumed to be in forced convection regime if the parameter suggested in Eq. (13) is less than 0.04. This criterion was investigated for our upward and

downward flow data. The results are presented in Figure 7, where the normalized Nusselt numbers obtained from the experiments were plotted against the Jackson's non-dimensional buoyancy parameter, Bu , from Eq. (13) for both upward and downward flows. The red, blue, and green data from here on correspond to the data for operating pressures of 7.5, 8.1, and 10.2 MPa respectively.

In the case of upward flow, three heat transfer regions were identified namely; regions I, II, and III as shown in Figure 7. In region I, the normalized Nusselt number (Nu) was almost linearly dependent on the buoyancy parameter and the flow can be characterized as the one close to the natural convection regime. In this region, Reynolds number was practically constant and hence, the change of Bu was mainly due to change of Gr_b . As a result of this, the linear decreasing trend of Nu with Bu in this region is a principle of natural convection [23]. As the T_b approaches the T_{pc} , the normalized Nu reaches a minimum value at Bu value of approximately 0.4. This is where the transition between regions I and II occurred and in terms of global view, this can also be viewed as the point where velocity profile is altered into an "M-shaped" velocity profile as discussed earlier. The minimum value of Normalized Nu was also observed to be dependent on the operating pressure. The transition from region I to II didn't occur along a single path but was dependent on the flow conditions as can be seen from wide scattering in region II especially for the lower operating pressure case. Bae *et al* [23] attributed this wide scattering to the thermal entrance length effects and flow history. As the T_b moves away from the T_{pc} , the transition from region II to III occurs and this is where the normalized Nu is independent of the Bu and the flow can be characterized as the one close to the forced convection regime. In this region, the Nu determined from the Jackson's correlation, Eq. (12), is the same as the experimental Nu .

In the case of downward flow, it can be expected that the buoyancy forces will enhance the turbulence production and hence, the normalized Nu should be greater than one for $Bu > 0.04$ [21]. This was found to be true for the present data as shown in Figure 7. It is interesting to note the region I for downward flow, where deterioration was observed, contrary to generally known belief that deterioration doesn't occur in a downward flow. Most of the data in this region is the data having T_b close to the T_{pc} and operating pressure of 7.5 MPa. Hence, this data can be classified as the deterioration data for downward flow due to the pseudo-film boiling phenomenon as discussed earlier. This deterioration was not observed for higher operating pressures as can be seen from gradual increase in wall temperature around the pseudocritical region in Figure 5. Excluding the region I, it can be safely assumed that the Normalized Nu monotonically increases with Bu .

Recently a global parameter based on Froude number (Fr) was developed by Seo *et al* [24] to study the influence of buoyancy.

$$\frac{1}{Fr} \sim \frac{1}{\rho_b} \left(\frac{\rho_b - \rho_w}{T_w - T_b} \right) \left(\frac{Q_{PS} D}{k_b} \right) \left(\frac{g D^3}{v_b^2} \right) \left(\frac{1}{Re_b^{2.8} Nu_b} \right) \quad (14)$$

It was suggested by Licht *et al* [25] that for inverse Froude number < 0.1 , the buoyancy effects are negligible. This criterion was verified using the current data for upward and downward flows. It has been found out that the criterion can satisfactorily predict the influence of buoyancy just like the Jackson's criterion for vertical flows.

For horizontal flows, Jackson [9] proposed a criterion to neglect the buoyancy effects and is in the form of,

$$Bo_j = \frac{Gr_b}{Re_b^2} \left(\frac{\rho_b}{\rho_w} \right) \left(\frac{x}{D} \right)^2 < 10 \quad (15)$$

This criterion was tested by plotting the normalized Nu versus the Bo_j for both the top and bottom sides of test section as shown in Figure 8. For the top side, two regions of heat transfer were identified namely; regions I and II. In the region I, the flow is dominated by natural convection and the change of Reynolds number was found to be relatively small compared to the change in Gr_b and normalized Nu was found to linearly increase with decrease in the Bo_j on a log-log plot. This linearly dependence can be used to develop a new correlation to predict the Nusselt number in buoyancy affected region for horizontal flows. Transition from region I to II occurs at Bo_j value of approximately 10 as suggested by Jackson [9]. In the region II, the T_b is greater than T_{pc} and the effects of buoyancy are minimized resulting in forced convection heat transfer. The normalized Nu in this region is independent of the Bo_j values and the Nu values predicted by the Jackson's correlation are nearly the same as the experimental values.

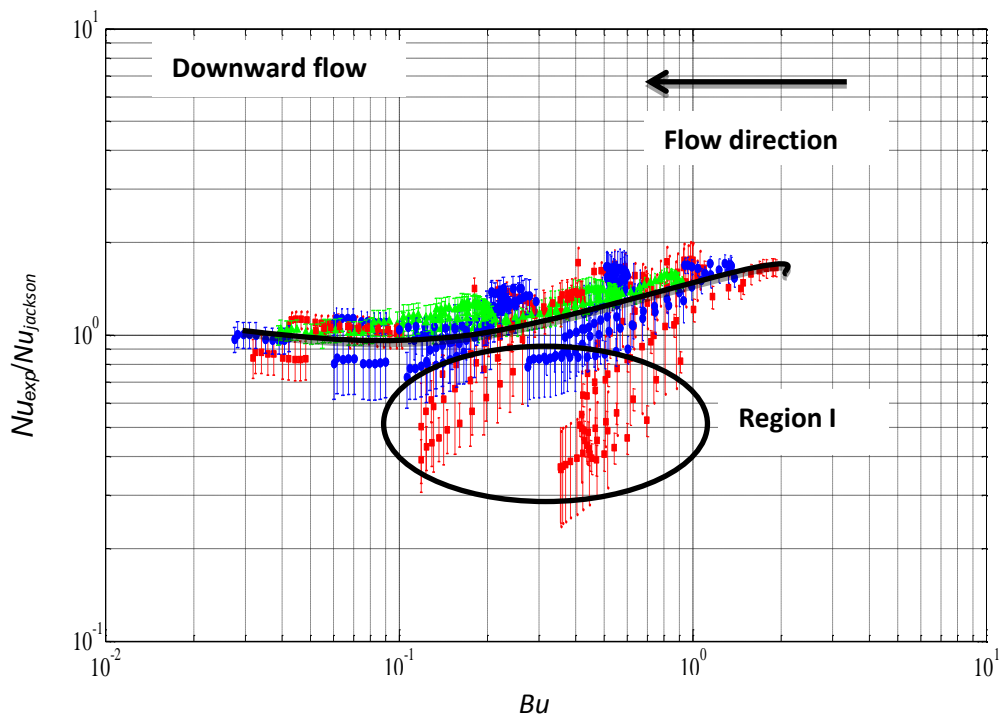
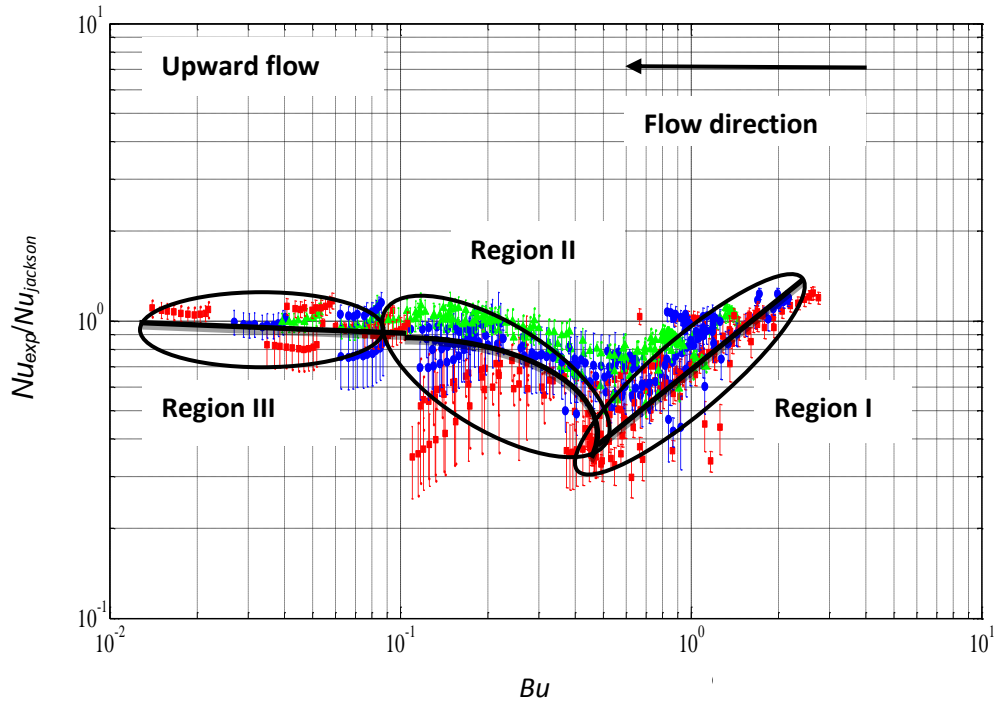


Figure 7. Normalized Nusselt number versus Jackson's buoyancy parameter, Bu

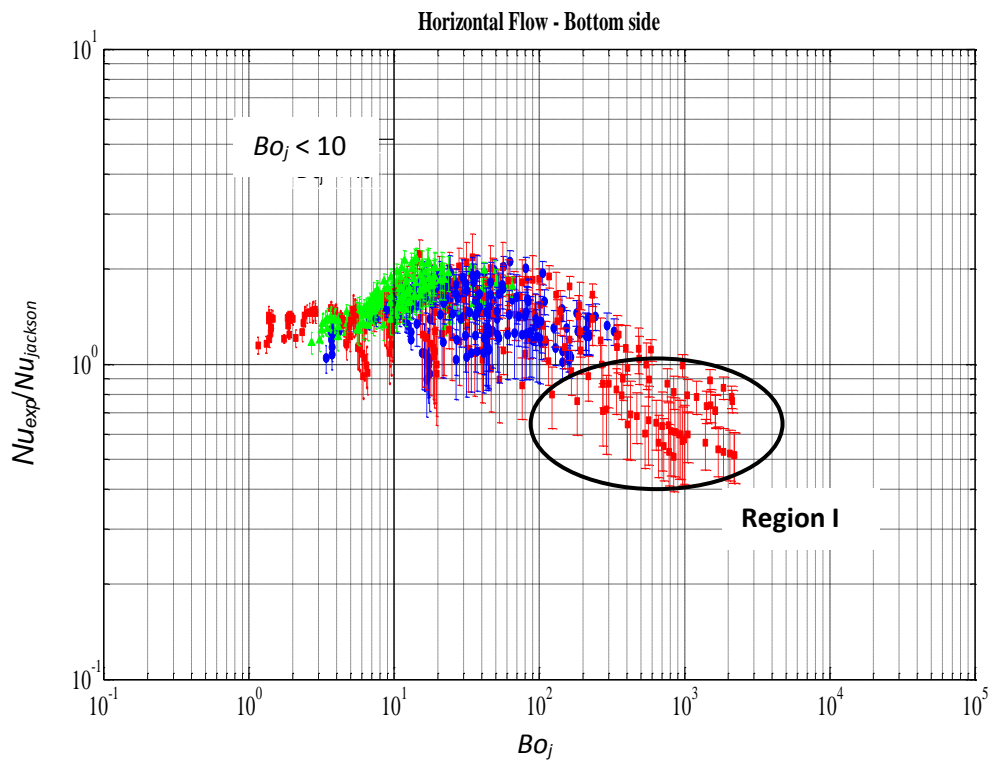
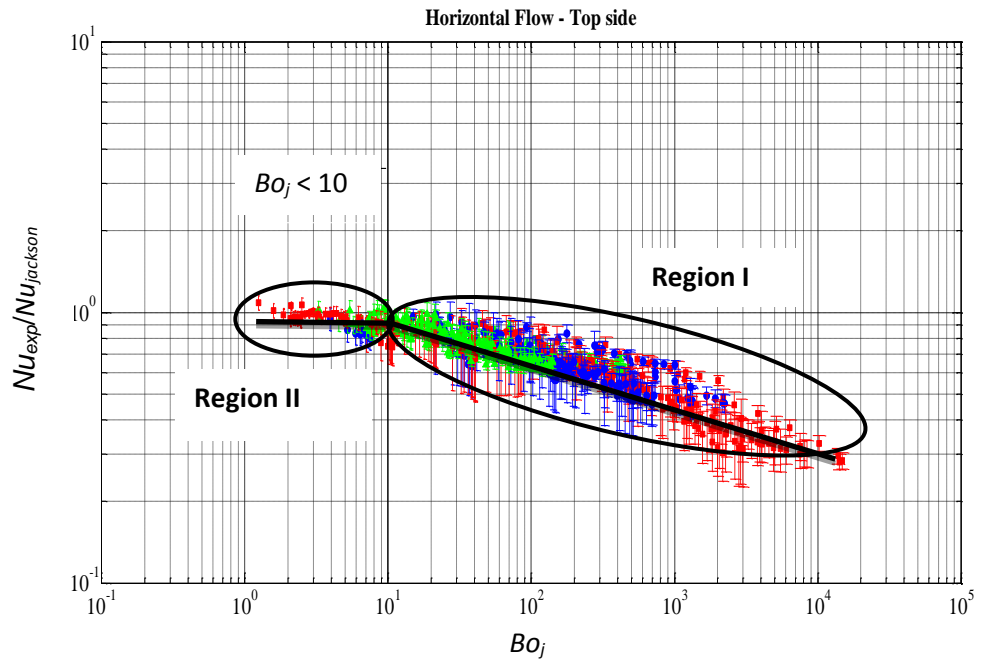


Figure 8. Normalized Nusselt number versus Jackson's buoyancy parameter, Bo_j

For the bottom side, no clear trend in normalized Nu was observed with respect to the Bo_j . However, for Bo_j value of less than 10, the normalized Nu values are approaching towards one. Similar to the downward flow, a region of deteriorated heat transfer was observed for the bottom side. This region, marked as region I, consists of data close to the pseudocritical region for operating pressure of 7.5 MPa. This can again be attributed to pseudo-film boiling phenomenon.

Petukhov *et al* [26] studied horizontal flows and derived a threshold value of Grashof number, Gr_{th} , above which the buoyancy effect can be neglected. Gr_{th} is defined as,

$$Gr_{th} = 3e - 5Re_b^{2.75} \overline{Pr}^{0.5} \left[1 + 2.4Re_b^{-\frac{1}{8}} \left(\overline{Pr}^{\frac{2}{3}} - 1 \right) \right] \quad (16)$$

Where,

$$\overline{Pr} = \frac{i_w - i_b}{T_w - T_b} \left(\frac{\mu_b}{k_b} \right)$$

They also defined a Grashof number based on heat flux as,

$$Gr_q = \frac{g \overline{\beta} Q_{PS} D^4}{v_b^2 k_b} \quad (17)$$

Where,

$$\overline{\beta} = \frac{1}{\rho_{film}} \left(\frac{\rho_b - \rho_w}{T_w - T_b} \right)$$

Petukhov *et al* [26] stated that the flow is completely dominated by forced convection for $Gr_q < Gr_{th}$. When this criterion was applied to the present data, no clear trend in the data was observed both for top and bottom sides. Although the criterion was not violated, Gr_q was found to be greater than Gr_{th} for all the data points indicating that the buoyancy cannot be neglected for any of the flow conditions. Hence, this criterion can be considered as stringent test for predicting the influence of buoyancy.

CONCLUSIONS

Systematic experiments were performed for horizontal, upward, and downward flows under similar conditions to understand the influence of buoyancy on heat transfer. When the bulk temperature is less than and the wall temperature is greater than the pseudocritical temperature, significant influence of buoyancy was observed for all three flow orientations. Enhancement and deterioration in the heat transfer was observed on the bottom and top sides respectively for horizontal flow leading to a circumferential variation in wall temperature. Turbulent shear stress was modified by buoyancy forces for both downward and upward flows. For upward flow, the buoyancy forces act to reduce the turbulent shear stress resulting in localized spikes in wall temperature. For downward flow, buoyancy forces act to enhance the turbulent shear stress enhancing the heat transfer compared to cases with no influence of buoyancy. The effect of buoyancy was observed to be most severe near the pseudocritical region and pressures closer to the critical pressure. When both the bulk and wall temperatures are above the pseudocritical temperature, effect of buoyancy was greatly minimized due to presence of more gas like CO₂ in both the bulk and near wall regions. Only mode of heat transfer deterioration for downward flow was observed to be due to the pseudo-film boiling phenomenon. Buoyancy parameters suggested in literature were investigated by normalizing the experimental Nusselt numbers with that of forced convection correlation suggested by Jackson and Hall. For vertical flows, the buoyancy criteria suggested by Jackson (Bu), and Seo *et al* ($1/Fr$) were able to correctly predict the influence of buoyancy on heat transfer. For horizontal flows, the buoyancy criterion suggested by Jackson (Bo_j) performed satisfactorily.

NOMENCLATURE

A	=	Area (m ²)
Bu	=	Jackson buoyancy parameter for vertical flows
C _p	=	Specific heat (KJ/Kg-K)
D	=	Diameter (m)
Fr	=	Froude number
g	=	Acceleration due to gravity (m/s ²)
G	=	Mass flux (Kg/m ² s)
h	=	Heat transfer coefficient (W/m ² .K)
i	=	Enthalpy (KJ/Kg)
k	=	Thermal conductivity (W/m.k)
L	=	Length (m)
\dot{m}	=	Mass flow rate (Kg/s)
Nu	=	Nusselt number
p	=	Pressure (bars)
Pr	=	Prandtl number, $\mu C_p/k$
\overline{Pr}	=	Prandtl number based on average C _p
Q	=	Heat rate (W)
Re	=	Reynolds number, $\frac{4\dot{m}}{\pi D \mu}$
T	=	Temperature (K)
x	=	distance from the end terminal

Greek symbols

β	=	volume expansion coefficient (K ⁻¹)
ρ	=	density (Kg/m ³)
μ	=	dynamic viscosity (Pa.s)
ν	=	kinematic viscosity, μ/ρ

Subscripts and Superscripts

av	=	averaged quantity of variable
b	=	mass averaged value
exp	=	experimental value
in	=	Inner or Inlet
out	=	Outer or Outlet
pc	=	Pseudocritical
ps	=	Power supply
ss	=	Stainless steel
w/wi	=	inner wall
wo	=	outer wall

REFERENCES

- [1] DoE, U. A technology roadmap for generation IV nuclear energy systems. in Nuclear Energy Research Advisory Committee and the Generation IV International Forum. 2002.
- [2] Dostal, V., P. Hejzlar, and M.J. Driscoll, The supercritical carbon dioxide power cycle: comparison to other advanced power cycles. Nuclear Technology, 2006. **154**(3): p. 283-301.
- [3] Liao, S. and T. Zhao, An experimental investigation of convection heat transfer to supercritical carbon dioxide in miniature tubes. International Journal of Heat and Mass Transfer, 2002. **45**(25): p. 5025-5034.

- [4] Incropera, F.P., A.S. Lavine, and D.P. DeWitt, Fundamentals of heat and mass transfer. 2011: John Wiley & Sons.
- [5] Kline, S.J. and F. McClintock, Describing uncertainties in single-sample experiments. Mechanical engineering, 1953. **75**(1): p. 3-8.
- [6] Belyakov, I., et al., HEAT-TRANSFER IN VERTICAL RISERS AND HORIZONTAL TUBES AT SUPERCRITICAL PRESSURE. Thermal Engineering, 1972. **18**(11): p. 55-&.
- [7] Yamagata, K., et al., Forced convective heat transfer to supercritical water flowing in tubes. International Journal of Heat and Mass Transfer, 1972. **15**(12): p. 2575-2593.
- [8] Bazargan, M., D. Fraser, and V. Chatoorgan, Effect of buoyancy on heat transfer in supercritical water flow in a horizontal round tube. Journal of heat transfer, 2005. **127**(8): p. 897-902.
- [9] Adebijiyi, G. and W. Hall, Experimental investigation of heat transfer to supercritical pressure carbon dioxide in a horizontal pipe. International Journal of Heat and Mass Transfer, 1976. **19**(7): p. 715-720.
- [10] Shitsman, M., Impairment of the heat transmission at supercritical pressures(Heat transfer process examined during forced motion of water at supercritical pressures). High temperature, 1963. **1**: p. 237-244.
- [11] Ackerman, J., Pseudoboiling heat transfer to supercritical pressure water in smooth and ribbed tubes. Journal of Heat transfer, 1970. **92**(3): p. 490-497.
- [12] Vikhrev, Y.V., Y.D. Barulin, and A. Kon'Kov, A study of heat transfer in vertical tubes at supercritical pressures. Thermal Engineering, 1967. **14**(9): p. 116-119.
- [13] Alferov, N., et al., Features of heat transfer due to combined free and forced convection with turbulent flow. Heat Transfer—Soviet Research, 1973. **5**(4): p. 57-59.
- [14] Jackson, J. and W. Hall, Influences of buoyancy on heat transfer to fluids flowing in vertical tubes under turbulent conditions. Turbulent forced convection in channels and bundles, 1979. **2**: p. 613-640.
- [15] Wood, R.D. and J. Smith, Heat transfer in the critical region—temperature and velocity profiles in turbulent flow. AIChE Journal, 1964. **10**(2): p. 180-186.
- [16] Bourke, P. and D. Pulling, An Experimental Explanation of Deterioration in Heat Transfer to Supercritical Carbon Dioxide. 1971: Atomic Energy Research Establishment.
- [17] Miropol'skiy, Z. and V. Baigulov. Investigation in heat transfer, velocity and temperature profiles with carbon dioxide flow in a tube over the nearly critical region of parameters. in Proceedings of the Fifth International Heat Transfer Conference. 1974.
- [18] Kurganov, V., V. Ankudinov, and A. Kaptilnyi, EXPERIMENTAL-STUDY OF VELOCITY AND TEMPERATURE-FIELDS IN AN ASCENDING FLOW OF CARBON-DIOXIDE AT SUPERCRITICAL PRESSURE IN A HEATED VERTICAL PIPE. High Temperature, 1986. **24**(6): p. 811-818.
- [19] Hall, W., J. Jackson, and A. Watson. Paper 3: A Review of Forced Convection Heat Transfer to Fluids at Supercritical Pressures. in Proceedings of the Institution of Mechanical Engineers, Conference Proceedings. 1967. SAGE Publications.
- [20] Shiralkar, B. and P. Griffith, The effect of swirl, inlet conditions, flow direction, and tube diameter on the heat transfer to fluids at supercritical pressure. Journal of heat transfer, 1970. **92**(3): p. 465-471.
- [21] Jackson, J., Fluid flow and convective heat transfer to fluids at supercritical pressure. Nuclear Engineering and Design, 2013. **264**: p. 24-40.
- [22] Jackson, J. and W. Hall, Forced convection heat transfer to fluids at supercritical pressure. Turbulent forced convection in channels and bundles, 1979. **2**: p. 563-611.

- [23] Bae, Y.Y., Mixed convection heat transfer to carbon dioxide flowing upward and downward in a vertical tube and an annular channel. *Nuclear Engineering and Design*, 2011. **241**(8): p. 3164-3177.
- [24] Seo, K.W., et al., Heat transfer in a supercritical fluid: classification of heat transfer regimes. *Nuclear technology*, 2006. **154**(3): p. 335-349.
- [25] Licht, J., M. Anderson, and M. Corradini, Heat transfer to water at supercritical pressures in circular and square annular flow geometry. *International Journal of Heat and Fluid Flow*, 2008. **29**(1): p. 156-166.
- [26] Petukhov, B., et al. Turbulent flow and heat transfer in horizontal tubes with substantial influence of thermo-gravitational forces. in *Proc. of Fifth Int. Heat Transfer Conference*. 1974.
- [27] Mokry, S., et al., Development of supercritical water heat-transfer correlation for vertical bare tubes. *Nuclear Engineering and Design*, 2011. **241**(4): p. 1126-1136.
- [28] Swenson, H., J. Carver, and C.d. Kakarala, Heat transfer to supercritical water in smooth-bore tubes. *Journal of Heat Transfer*, 1965. **87**(4): p. 477-483.
- [29] Bishop, A., R. Sandberg, and L. Tong, Forced-convection heat transfer to water at near-critical temperatures and supercritical pressures. 1964, Westinghouse Electric Corp., Pittsburgh, Pa. Atomic Power Div.

ACKNOWLEDGEMENTS

This work was performed under NEUP grant 11-3039 from U. S. Department of Energy (DOE).